



# An automatic MRI brain image segmentation technique using edge–region-based level set

Nasser Aghazadeh<sup>1</sup> · Paria Moradi<sup>1</sup> · Giovanna Castellano<sup>2</sup> · Parisa Noras<sup>1</sup>

Accepted: 9 November 2022 / Published online: 27 November 2022

© The Author(s), under exclusive licence to Springer Science+Business Media, LLC, part of Springer Nature 2022

## Abstract

Digital transformation has brought radical changes in several domains. Particularly, image processing techniques have been generally used in medical, security, and monitoring applications. Image segmentation is a specific task where an image is partitioned in meaningful segments, containing similar features and properties. Its aim is to simplify the original image for easy analysis since relevant information is highlighted. These techniques are commonly used to support medical experts in detecting areas of interest in medical images. Level set method is a methodology for image segmentation, which works with minimizing energy for segmentation of the image by active contours. The areas inside each contour belong to distinct segments. In active contour-based models, the level of each contour changes according to the intensity values (region-based active contours) or the gradient variations (edge-based active contours). Here, a new edge–region level set algorithm for image segmentation is proposed which controls the curve movement based on both intensity and gradient values. Moreover, the original active contour model has been modified by considering both the mean and the variance values of the pixels' neighborhood, instead of the mean value only. Indeed, in homogeneous regions with the same mean value could be assigned to the same segment while belonging to different ones. Since the initial curve definition is crucial for level set methods, a new methodology for initial curve detection based on Canny edge detector has been proposed. Experiments have been conducted on brain tumor magnetic resonance imaging (MRI). Images from Whole Brain Atlas (Harvard University Medical School) datasets, part Neoplastic Disease (brain tumor) have been used. Results have shown that the suggested approach is able to accurately detect tumor regions in the images and to overcome the original active contour models such as CV, LBF, and LIF. Using semi-average filter in pre-processing stage can strengthen edges and it led to detecting more strong edges in Canny edge detector.

**Keywords** Image segmentation · Level set · Mean · Variance · Medical images · MRI

## 1 Introduction

The brain tumor is rarer, with respect to other types of cancer, but it has a potentially fatal effect on the patient. The most common and current brain tumors are gliomas which affect the glial tissue of the nervous system. Gliomas are commonly classified into three types, depending on the histological appearance, namely astrocytic, oligodendroglial or ependymal tumors [1]. Tumors belonging to different groups have different natural histories, responses to treatment, and outcomes, thus timely detection of the tumor, and its type identification is crucial for the patient.

Magnetic resonance imaging (MRI) is the standard medical imaging technique used for identifying brain tumors. MRI is a noninvasive approach since it benefits magnetic fields and radio waves to attain images of the organs in the body [2]. MRI can be combined with other methodologies, e.g., computed tomography (CT), positron emission tomography (PET), or magnetic resonance spectroscopy (MRS) to extract specific information on the tumor morphology and metabolism. However, even if extra information can be provided by these technologies, the accepted standard for brain tumor imaging is still MRI. Thus, in this paper, we will focus on MRI images.

MRI scans of the brain are used by medical experts for the diagnosis and treatment of the pathology. MRI analysis is commonly manually performed by specialists. This task other than being boring makes the outcome subjective. Indeed, different experts could interpret the images based on their experience. For this reason, in recent years, biomedical image processing techniques have been used for automating the analysis of brain tumor MRI scans, to support medical experts [3]. Several machine learning techniques have been proven to be efficient in the automatic detection of brain tumors through MRI [4]. Particularly, deep learning algorithms are generally used in medical applications for the early detection of disease [5, 6]. However, these methods require huge amounts of data to train their models.

Image segmentation is still a wide and important field of research in medical science, due to its capability of automatically partitioning brain images into non-overlapping meaningful regions, corresponding to some physical properties like pixel intensity, texture, and homogeneity. This leads to image segments differing in materials they are composed of various tumor tissues [3]. In addition, the tumor cell shape, distribution, and position are used to define tumor morphological and phenotypic profiles, which are used for diagnosing and designing effective treatment strategies.

However, image segmentation of brain scans is difficult to work. This is mainly because of the complexity of the human brain, but it also depends on technical issues related to image acquisition such as noise, partially occluded regions, missing edges, and lack of texture contrast between interest regions and background.

Several image segmentation techniques have been proposed [7–14]. They can be categorized into two main approaches, namely *region based* [15, 16] and *edge based* [17, 25]. Region-based methods are robust because unlike edge-based

methods that distinguish only edges to define segmentation regions, these region-based methods identify more pixels in addition to edges to detect regions. In addition, we can use, for example, in addition to the edges, the texture of the image to detect regions. In edge-based methods, first- or second-order derivatives are used for detecting the boundary of the images [26–28].

The edge-based forms usually use image gradients for extracting contours in object boundaries, and they can return accurate results for edge-based segmentation problems. The Canny edge detector is accurate and fast; therefore, it can be used in the edge detection of images. The edge-based forms are convenient for images with strong and clear boundaries and are sensitive to initial information and noise. Therefore, they return low achievement for images with weak edges. On the contrary, since region-based forms use statistical information about pixels outside and inside closed contours, for image segmentation, they are less sensitive to noise, with respect to edge-based approaches, and they are also able to return accurate results for images with weak boundaries.

Active contour (snake) models which are stable image segmentation methods allocate closed boundaries and they are efficient. The main concept of active contour models is to apply the partial differential equations to iteratively evolve the initial contours, toward the boundaries of objects. This is done by minimizing an energy functional which is given [29, 30], based on the contour energies, inside and outside the regions. Using an initial contour, the external energies stimulate the progress of a parametric active contour model while the internal energies manage the shape of the given contour. However, the initial curve definition in the active contour model is important. Indeed, the use of a not suitable initial curve could lead to not accurate segmented regions.

A novel automatic MRI brain image segmentation technique according to the level set algorithm has been presented in this study. We have examined this scheme on MRI tumor brain images by using level set together with Canny edge detector. At first, this method discovers the initial contour that comes from normalization, thresholding, and Canny Edge detector. The mask is built from thresholding and the image is reconstructed. The initially given contour is approximated by the boundary of the eroded mask. The level set technique segments the desired region by using the given initial contour. In the proposed algorithm, the sum of mean values and the variance values have been used for controlling contour movement in contrast to the original active contour model which uses only mean value. Using variance value, led to accurate segmentation of regions. We deform the boundary to the nearest Canny edges to improve the accuracy of the extracted boundary of the initial curve. Then, we use it as an initial curve in the presented level set model. Experiments and tests were conducted on a large number of images from *Whole Brain Atlas dataset, Neoplastic Disease (brain tumor)* part.<sup>1</sup> Numerical results have shown that the presented pipeline is accurate in segmenting regions of tumor and it obtains more accurate results than the original active contour model algorithm. Moreover, a main finding of this paper is the automatic detection of the initial contour by the Canny

<sup>1</sup> <https://www.med.harvard.edu/aanlib/home.html>

edge method. Indeed, in the original active contour model, the initial contour needs to be set manually. This is time-consuming other than not accurate segmentation results may be obtained.

The article is organized as follows. In Sect. 2, we discuss the state-of-the-art methods for image segmentation, by highlighting their strengths and weaknesses and how the presented technique can dominate their limits. Section 3 elaborates on the presented approach. Both quantitative and qualitative results are reported in Sect. 4. The Conclusion is presented in Sect. 5.

## 2 Related works

A formal definition of a segmentation task of an image  $S$  is a finite set of regions  $S_1, S_2, \dots, S_n$  which the following conditions are satisfied:  $S = \cup S_i$  and  $S_i \cap S_j = \emptyset$  for ( $i \neq j$ ).

Segmentation approaches can be grouped in region based and edge based. In the region-based approaches, similar features of the pixels are used for segmentation. Particularly, these methods aim to detect homogeneous regions in the images, based on several pixel characteristics, such as grayscale, color, texture, or any other pixel-based measures. Pixels with alike attributes are grouped in one region  $I_i$ . It should be noted that the choice of the homogeneity criteria is a main factor that affects the segmentation results. The following conditions are fulfilled when an image  $S$  is segmented by region-based approaches:

1. All regions  $S_i$  should be homogeneous subject to some particular criteria:  $H(S_i) = \text{true}$ ,  $i = 1, 2, \dots, S$ .
2. The region that emerges by merging two adjacent regions  $S_i$  and  $S_j$  is not homogeneous:  $H(S_i \cup S_j) = \text{false}$ .

Edge-based segmentation methods are exploited to detect intensity changes which lead to spotting edges in the image. The edge and the gradient magnitudes coincide for certain points in the image, and the gradient direction is used to detect the edges. Therefore, with the aid of first- and second-order derivatives, changes in intensity can be detected. Various edge detection operators have been proposed, which are based on weights collections applied to the pixel and its neighbors. Operators are generally displayed through rectangular masks or filters with sets of weights. Masks are then applied to the image, to segment it, by utilizing discrete convolution. The simplest segmentation approach for edge-based segmentation is the use of a threshold  $\lambda$  applied to pixels intensity for separating objects from the background. Otsu's method is a significant and practical threshold technique [18].

In this paragraph, we attempt to briefly describe the most relevant segmentation approaches. MRI images are non-homogeneous and have poor contrast and because of that by hand tumor detection in MRI scans is difficult. So, using some automatic methods for tumor detection is necessary [19]. There are several methods for segmenting the region of tumor such as using threshold [20, 21], neural network [22],

fuzzy C-means [23], and DWT [24]. But the classic methods such as watershed and thresholding due to using less information can't segment the region exactly, and thresholding doesn't use the texture of the images. Using DWT, fuzzy C-means, and neural networks leads to better results and exact tumor regions rather than classic methods, but they need more features and more time for processing. Several active contour-based algorithms have been developed. The Mumford–Shah model [25] is one of the universally used mathematical models for image segmentation. Chan and Vese have then modified this method by using the level set formulation, which leads to a simpler approach to solving the problem [31]. Indeed, a piecewise smooth approximation is used instead of a constant approximation. Osher and Sethian developed a new model that can exploit the classes based on Hamilton–Jacobi formulations. [32]. Vese extended the multiphase case of [2] model in 2001. Recently many models have been developed by extending the Chan and Vese's model. In [46] Li, et al. proposed an energy function, based on K-means clustering algorithm. Recently, Li et al. suggested the local binary fitting (LBF) model, by defining a kernel function to display image information in local regions. LBF model has been shown to outperform Mumford–Shah and Chan–Vese models (CV) in segmenting images by considering intensity inhomogeneity. A further improvement has been proposed, where the region-scalable fitting (RSF) model is used to develop the performance of image segmentation with intensity inhomogeneity [48]. This method used local intensity information with a controllable scale to construct an energy functional model. Ali et al. [33] extended a variational model to deal with regions with intensive inhomogeneities. Mabood et al. [35] introduced an absolute median deviation-based model for noisy images, which is more effective compared to the local Chan–Vese (LCV) model [34]. Zhang et al. [36] developed the CV model by using the local binary fitting (LBF) energy and local image fitting (LIF) energy. More related models have been introduced in [37–40] by defining energy functional based on some information, e.g., prior shape information [41–43]. With suitable curve initialization and input parameters set, these models can well extract the objects on images, but with usually complex estimation approaches.

Even if all these methods have been proven to be effective in image segmentation, they also present some weaknesses such as the presence of noise in the results or the influence of the initial curve on the results. To overcome these limitations, here, we introduce an active contour technique that collects the properties of both edge-based active contour models and region-based active contour models. This method can detect a suitable initial curve for the level set to speed the process of segmentation. Moreover, to increase the accuracy, mean and variance have been used, inside and outside the edges, instead of mean value only. Adding variance to mean values of the regions can lead to separate regions better than using only mean values of the regions. Previous active contour-based methods work well in homogeneous regions and in this case, using mean values of the regions can lead to good segmentation results. In this work, by adding variance, the boundary of regions can be detected exactly specially in the case of inhomogeneous regions. In the case of computational complexity, it is true that by adding variance, the number of operations increases, but by the automatic setting of the initial curve via Canny edge detection, the speed of the proposed algorithm accelerates.

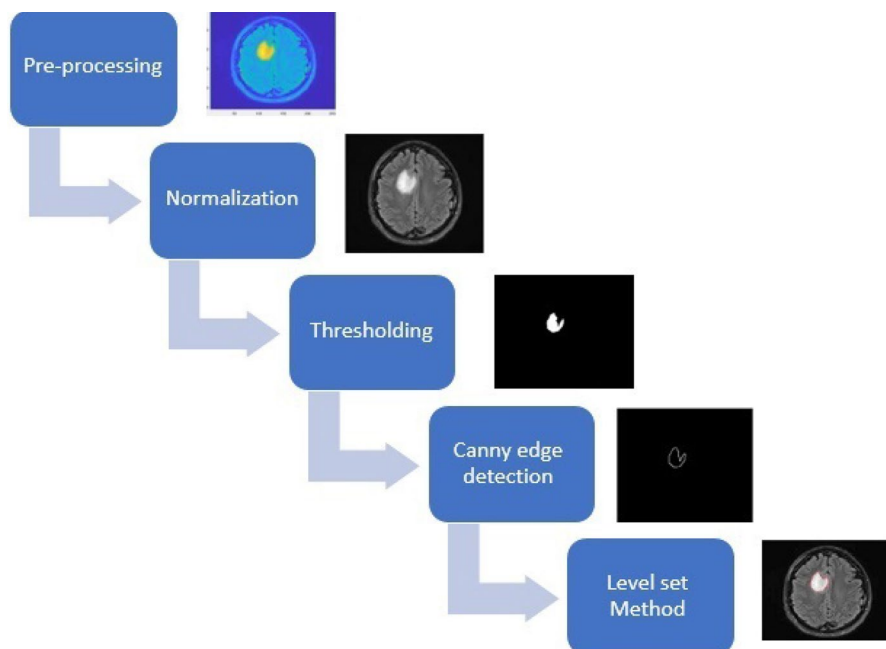


**Fig. 1** Flow diagram of the proposed model

The highlights of this paper are:

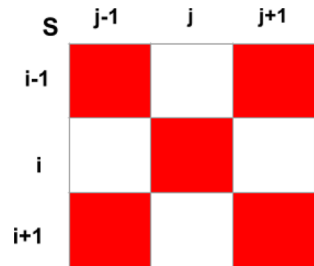
1. A new segmentation method has been proposed, that can effectively deal with inhomogeneity intensity in MRI brain images.
2. A pre-processing phase is proposed where a filter is used for reducing noise and artifacts effect, other than for sharpening the edges.
3. Mean and variance are combined in the level set algorithm to improve its sensitivity.

### 3 Proposed model for MRI brain image segmentation

Here, a new algorithm for MRI scan segmentation of brain tumors is introduced.

It is clear from Fig. 1 that the proposed region–edge-based method for segmentation, is composed of five main steps that from raw MRI scans lead to segmented images, namely:

1. *Pre-processing* semi-average filter is applied to raw MRI scans to remove noise and artifacts.
2. *Normalization* *min–max* scaling is applied to each feature describing each pixel, in order to reduce differences in scales.

**Fig. 2** Semi-average filter

3. *Thresholding* a threshold is applied to separate region of interest from background.
4. *Canny edge detector* it is applied to extract edges from the image.
5. *Level set* It is used for moving initial contour into boundaries of the region.

### 3.1 Pre-processing

Raw MRI scans often contain extra information such as noise or artifacts that affect relevant regions' identification. In order to either decrease or eliminate the effects of this extra information from MRI images, filtering algorithms are commonly applied. Mean filtering is the most widely used technique that is able to remove distortion and artifacts without losing features. It is based on the reduction of the intensity variation between one pixel and its neighbors, which leads in a reduction of the noise in images. Each pixel in an image is replaced with the averaged values of its neighbors. This process smooths the image by reducing the influence of pixels that are not representative of their surroundings. Often a  $3 \times 3$  square kernel is used to define the neighborhood of each pixel. However, the main drawback of mean filtering is that when not homogeneous regions occur, the accuracy of the identified regions could decrease, because some pixels could be considered within neighbors while showing some differences. So in this article, a new semi-average filter is proposed, where a  $3 \times 3$  square kernel is considered, but only pixels on the main diagonal are averaged, as displayed in Fig. 2. Thus, the first step of the proposed pipeline applies the semi-average filter to raw images to reduce the noise, as follows:

Let  $S_1(i, j)$  be a pixel in the original MRI image the pre-processed output representing the filtered image is given by:

$$S_2(i, j) = \text{Mean}\{S_1(i-1, j-1), S_1(i-1, j+1), S_1(i, j), S_1(i+1, j-1), S_1(i+1, j+1)\} \quad (1)$$

Using proposed semi-average filter led to highlight edge regions in diagonals.

### 3.2 Normalization

In the second step of the proposed pipeline, *min-max* scaling is applied to images.

First, suppose that each image  $X$  can be represented as the set of the data points (pixels) in it,  $X = \{x_1, x_2, \dots, x_n\}$  ( $1 \leq i \leq n$ ) where  $n$  is the number of pixels in the image. Given  $[x^{\min}, x^{\max}]$  the range of the pixels, then each pixel  $x_i$  is normalized using the following equation

$$x_i = \frac{x_i - x^{\min}}{x^{\max} - x^{\min}}. \quad (2)$$

In this way, all the pixels values, represented by the gray scale, have been re-scaled in the same interval  $[0, 1]$ , so as they can be comparable.

### 3.3 Thresholding

A threshold  $\lambda$  is used to extract the regions of interest. Particularly, all data points having higher values than  $\lambda$  are considered as interior points foreground and they are assigned to our region of interest. The remaining points are considered to be outside the region of interest, thus they are assigned to the background. A soft threshold, which is defined as follows, has been used:

$$FB = \text{sign}(F) || F | - \lambda | \quad (3)$$

where  $F$  is the input image and  $FB$  is the output image after the thresholding process. We have preferred soft threshold, to a crisp one, since the intensity changes in the brain images are not sharp and they change smoothly. Thus, soft threshold is more suitable to better capture different regions, while reducing the errors.

### 3.4 Canny edge detector

In the fourth step of our pipeline, edges in the image are detected. To this aim, the Canny edge detector has been used [49]. It is the more powerful edge detection method and consists of four steps. Smoothing the image by a Gaussian filter with a given standard deviation  $\sigma$ , is the first step. In the second step, by the use of any first-order operator, the derivatives in both directions are computed. It contains wide ridges around the local maxima of the gradient and it shows the typicality of the gradient magnitude of the image. It is imperative for local maxima to be marked as edges, because only then it would be possible to obtain a single response to an edge. This is known as *non-maxima suppression* (see, e.g., [51]). As a first step in performing non-maxima suppression, the edge directions are quantized according to 8 or 4 connectivity. Then, a candidate edge pixel with a greater magnitude than zero (magnitude  $> 0$ ) is considered. Candidate edge pixels are then compared with their neighboring pixels, both in edge and opposite direction, to determine whether a candidate edge pixel should be marked for deletion or not. Therefore, all the candidate edge pixels with a magnitude that is lower than the one of their neighboring pixels are marked for deletion. In order to delete lines or pixels with no continuous edge, hysteresis thresholding is used. In addition to the mentioned results, the derivative operator that is utilized to find the magnitude, and



the non-maxima suppression implementation, are also effective on the final edge segmented image.

### 3.5 Level set

Osher and Sethian in [16] presented an efficient and effective definite model for ongoing curves and surfaces, with a wide range applications, since the automatic change of topology authorizes there, such as merging and breaking. Also, the calculations are constructed on a fixed rectangular lattice. In the technique of level set, an ongoing curve  $C$  is displayed by the zero level set of a function  $\Phi : \Omega \rightarrow \mathbb{R}$  that satisfies Lipschitz condition. Then,  $C = \{(x, y) \in \Omega : \Phi(x, y) = 0\}$ , where  $S$  is the original image and  $\Phi$  has positive values inside  $C$  and negative values outside it. Here, for the formulation of the level set for our variational active contour model we pursue the methodology proposed in ([49]). Then, we change the variable  $C$  with the variable  $\Phi$  and the new energy notation  $F(\phi, c_1, c_2)$ , became unchanged. Thus, the equation turns into:

$$\begin{aligned} F(\phi, c_1, c_2) = & \mu \text{length}\{\phi = 0\} + \nu \text{area}\{\phi \geq 0\} \\ & + \lambda_1 \int_{\phi \geq 0} |S - c_1|^2 dx dy \\ & + \lambda_2 \int_{\phi < 0} |S - c_2|^2 dx dy \end{aligned} \quad (4)$$

which  $\mu$  and  $\nu$  are constant parameters with positive or zero values. Values of  $\lambda_1$  and  $\lambda_2$  influence the given weight to the regions, they usually are assumed as unity.  $\text{length}\phi = 0$  is the length of curve/contour and  $\text{Area}\phi \geq 0$  is the area of the image  $u$ .

This formulation will match the Mumford–Shah model if  $\nu = 0$  and  $\lambda_1 = \lambda_2$  and the constants  $c_1$  and  $c_2$  are replaced by piecewise smooth approximations.

Using the Heaviside function  $H$  and the Dirac measure  $\delta$ :

$$\delta(x) = \frac{d}{dx} H(x), \quad (5)$$

the terms in the energy  $F$  can be showed by:

$$\begin{cases} \text{length}\{\phi = 0\} = \int_{\Omega} |\nabla H(\phi)| = \int_{\Omega} \delta(\phi) |\nabla \phi|, \\ \text{area}\{\phi \geq 0\} = \int_{\Omega} H(\phi) dx dy, \end{cases}$$

and

$$\begin{cases} \int_{\phi \geq 0} |S - c_1|^2 dx dy = \int_{\phi \geq 0} |S - c_1|^2 H(\phi) dx dy, \\ \int_{\phi < 0} |S - c_2|^2 dx dy = \int_{\phi \geq 0} |S - c_2|^2 (1 - H(\phi)) dx dy, \end{cases} \quad (6)$$

So  $F(\phi, c_1, c_2)$  may be expressed as:

$$\begin{aligned}
F(\phi, c_1, c_2) = & \mu \int_{\Omega} \delta(\phi) |\nabla \phi| + \nu \int_{\Omega} H(\phi) dx dy \\
& + \lambda_1 \int_{\Omega} |S - c_1|^2 H(\phi) dx dy \\
& + \lambda_2 \int_{\Omega} |S - c_2|^2 (1 - H(\phi)) dx dy
\end{aligned} \quad (7)$$

By supposing  $\phi$  to be fixed and by minimizing  $F(\phi, c_1, c_2)$  subject to the  $c_1$  and  $c_2$ , it is simple to display these constants function of  $\phi$  by:

$$c_1(\phi) = \frac{\int_{\Omega} S H(\phi) dx dy}{\int_{\Omega} H(\phi(x, y)) dx dy} \quad (8)$$

and

$$c_2(\phi) = \frac{\int_{\Omega} S(1 - H(\phi)) dx dy}{\int_{\Omega} (1 - H(\phi(x, y))) dx dy} \quad (9)$$

where  $c_1$  is the average of  $u_0$  in  $\{\phi \geq 0\}$  and  $c_2$  is the average of  $u_0$  in  $\{\phi < 0\}$ . [45] By supposing that the  $c_1$  and  $c_2$  are fixed, and by minimizing the energy subject to  $\phi$ , we get the famous Euler–Lagrange equation for  $\phi$ :

$$\frac{\partial \phi}{\partial t} = \delta(t) \left[ \mu \operatorname{div} \left( \frac{\nabla \phi}{|\nabla \phi|} \right) - \nu - \lambda_1 (S - c_1)^2 + \lambda_2 (S - c_2)^2 \right] \frac{\partial \Omega}{|\nabla \phi|} \frac{\partial \phi}{\partial n} = 0. \quad (10)$$

We have to in practice, assume a little regularized exemplars of the functions  $H$  and  $\delta$  denoted here by  $H_{\varepsilon}$  and  $\delta_{\varepsilon}$ , where  $\delta_{\varepsilon}(x) = H'_{\varepsilon}(x)$ . For instance, a regularization by  $C^2$  and, respectively,  $C^1$  functions is:

$$H_{1,\varepsilon}(x) = \begin{cases} 1, & x > \varepsilon; \\ 0, & x < -\varepsilon; \\ \frac{1}{2} \left[ 1 + \frac{x}{\varepsilon} + \frac{1}{\pi} \sin\left(\frac{\pi x}{\varepsilon}\right) \right], & |x| \leq \varepsilon. \end{cases} \quad (11)$$

and

$$\delta_{1,\varepsilon}(x) = H'_{1,\varepsilon}(x) = \begin{cases} 0, & |x| > \varepsilon; \\ \frac{1}{2\varepsilon} \left[ 1 + \cos\left(\frac{\pi x}{\varepsilon}\right) \right], & |x| \leq \varepsilon. \end{cases} \quad (12)$$

which represented in [44].

In Chan–Vese algorithm [45], the authors regularized the Heaviside function used in (6) and (7):

$$H_{2,\epsilon}(x) = \frac{1}{2} \left( 1 + \frac{2}{\pi} \arctan\left(\frac{x}{\epsilon}\right) \right) \quad (13)$$

and they defined the delta function as its derivative:

$$\delta_{2,\epsilon}(x) = H'_{2,\epsilon}(x) = \frac{1}{\pi} \frac{\epsilon}{\epsilon^2 + x^2}. \quad (14)$$

In this work, we present and use in the examples this  $C^\infty(\Omega)$  regularization of  $H$

$$H_{2,\epsilon}(x) = \frac{1}{2} \left( 1 + \tanh\left(\frac{x}{\epsilon}\right) \right) \quad (15)$$

and the delta function as its derivative which is defined as:

$$\delta_{2,\epsilon}(x) = H'_{2,\epsilon}(x) \quad (16)$$

$$\begin{cases} M_1(\phi(x)) = H(\phi(x)), \\ M_2(\phi(x)) = 1 - H(\phi(x)), \end{cases} \quad (17)$$

Moreover, in our method, we replace the mean value of inside and outside of each contour by the sum of mean values and variance values. The reason of this idea is that some regions with the same mean values may have different variance values. We have used this fact for moving contours in active contour model. Then, our energy function  $F(\phi, c_1 + \sigma_1, c_2 + \sigma_2)$  can be displayed as:

$$\begin{aligned} F(\phi, c_1 + \sigma_1, c_2 + \sigma_2) &= \mu \int_{\Omega} \delta(\phi) |\nabla \phi| + \nu \int_{\Omega} H(\phi) dx dy \\ &\quad + \lambda_1 \int_{\Omega} \|S - c_1 - \sigma_1\|^2 (M_1(\phi(x)))^2 dx dy \\ &\quad + \lambda_2 \int_{\Omega} \|S - c_2 - \sigma_2\|^2 (M_2(\phi(x)))^2 dx dy \end{aligned} \quad (18)$$

In this paper, we suppose that  $\nu = \mu = 0$ , so our model can be displayed as:

$$\begin{aligned} F(\phi, c_1 + \sigma_1, c_2 + \sigma_2) &= \lambda_1 \int_{\Omega} \left\{ \frac{1}{2} (1 + \tanh(\frac{x}{\epsilon})) \right\}^2 \|S - c_1 - \sigma_1\|^2 dx dy \\ &\quad + \lambda_2 \int_{\Omega} \left\{ \frac{1}{2} (1 - \tanh(\frac{x}{\epsilon})) \right\}^2 \|S - c_2 - \sigma_2\|^2 dx dy \end{aligned} \quad (19)$$

where  $u_0$  is a given image,  $\Omega$  is domain, and  $\lambda_1, \lambda_2$  are parameters which balance the influences of the terms in the model. Moreover,  $c_1(\phi) = \text{average}(S)$  in  $\phi \geq 0$  and  $c_2(\phi) = \text{average}(S)$  in  $\phi < 0$ . As  $\epsilon \rightarrow 0$ , the approximation  $H_{2,\epsilon}(\phi) = \frac{1}{2}(1 + \tanh(\frac{x}{\epsilon}))$  converges to the Heaviside function ( $H(\phi) = 1$ , if  $\phi \geq 0$  and  $H(\phi) = 0$ , if  $\phi < 0$ ) as in [31]. For the computational stability, we used the square of  $H$  in our model.

The first term forces  $\{\frac{1}{2}(1 + \tanh(\frac{x}{\epsilon}))\}^2$ , toward 0 if  $S$  is different from  $c_1$  and toward 1 if  $S$  is close to  $c_1$  for each  $x \in \Omega$ . In a similar way,  $\{\frac{1}{2}(1 - \tanh(\frac{x}{\epsilon}))\}^2$ , toward 0 if  $u_0$  is different from  $c_2$  and toward 1 if  $S$  is close to  $c_2$ , for every  $x \in \Omega$ .

Figures 3 and 4 show the results of three MRI image segmentation. They represent tumorous brains with three-phase level set that uses from  $H_{2,\epsilon} = \{\frac{1}{2}(1 + \frac{2}{\pi} \arctan(\frac{x}{\epsilon}))\}$  and with  $H_{2,\epsilon} = \{\frac{1}{2}(1 + \tanh(\frac{x}{\epsilon}))\}$ . The suggested approximation of  $H$  works better than the previous one.

## 4 Results and discussion

A pipeline for automatic MRI brain image segmentation, using the level set algorithm has been presented in this study. The efficiency of the presented approach in segmenting MRI scans has been evaluated on Harvard university datasets [50] dataset. A twofold experimentation has been conducted. We have firstly evaluated the efficiency of the presented approach in correctly detecting segments of images. Thus, qualitative and quantitative experiments have been carried out. Furthermore, our approach has been compared with baseline segmentation methods.

In Figs. 3 and 4, it can be seen that the proposed method can detect white regions which are related to tumor regions, better than previous level set method.

### 4.1 Quantitative evaluation

In order to quantitatively evaluate our method, the following measures have been used. Dice similarity coefficient (DSC), accuracy, and sensitivity, along with the computational time required by the algorithm, have been used to evaluate the efficiency of the presented approach.

DSC is a useful summary measure of spatial overlap between the ground truth and foreseen value. Mathematically, this can be stated as

$$\text{DSC} = \frac{2 * TP}{(TP + FP) + (TP + FN)} \quad (20)$$

where  $TP$  shows the number of subjects correctly identified as affected by tumor.  $FP$  shows the number of subjects that have been identified as affected by tumor, but are healthy.  $TN$  shows the number of subjects correctly identified as belonging to the healthy class.  $FN$  indicated the false negatives, that is the subjects that are affected by tumor but have been identified as healthy.

Sensitivity measures the algorithm capability of detecting the target classes (tumor). So, sensitivity is the rate of true positives that prove the capability of the method in correctly predicting the tumorous brain tissues. Mathematically, this can be stated as:

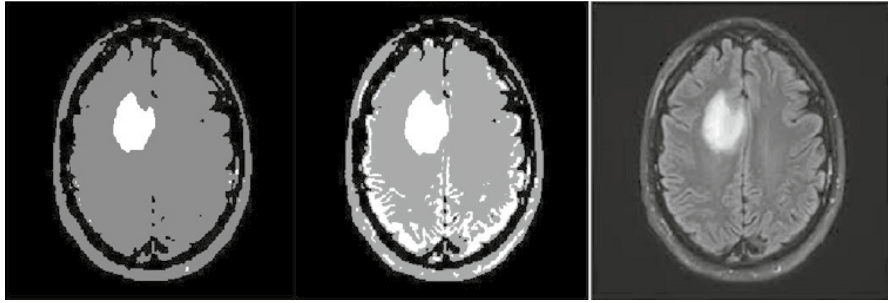


**Fig. 3** From left to right: The first image is the segmented image by proposed level set model into three regions which is presented by three colors, the second one is the segmented image by previous level set model into three regions which is presented by three colors, the third one is the original image

$$\text{Sensitivity} = \frac{TP}{TP + FN}. \quad (21)$$

Accuracy is the ability to distinguish among the patient affected by the disease and the healthy cases, accurately. Mathematically, this can be stated as:

$$\text{Accuracy} = \frac{TP + TN}{TP + TN + FP + FN}. \quad (22)$$

The performances values have been obtained on some images from *Whole Brain Atlas* (Harvard University Medical School) datasets. Here, we put  $\nu = \mu = 0.1$ ,  $\lambda_1 = 10$ ,  $\lambda_2 = 100$ . The proposed method has been implemented and executed in Matlab 2017. The proposed method has reached an accuracy of 0.988, a sensitivity of 0.978, and DSC of 0.997. These values suggest that the proposed approach is promising.

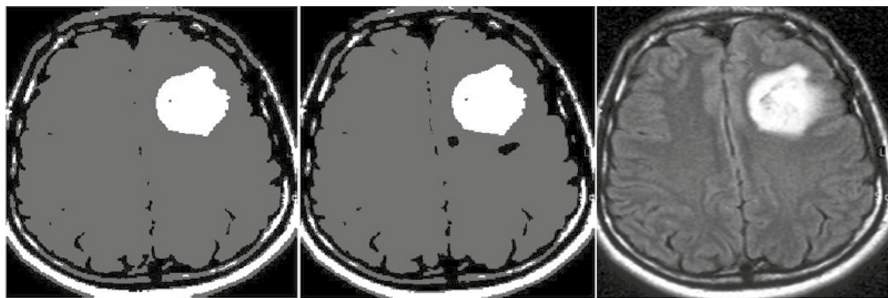


**Fig. 4** From left to right: The first image is the segmented image by proposed level set model into three regions which is presented by three colors, the second one is the segmented image by previous level set model into three regions which is presented by three colors, the third one is the original image

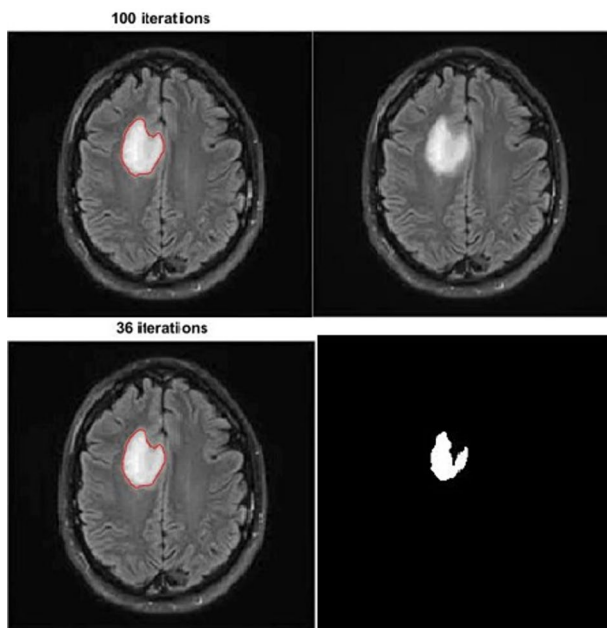


**Fig. 5** Original image (top left), the result of 100 iteration (top right), the result of initial curve of our method (bottom left), the result of 36 iteration (bottom right)

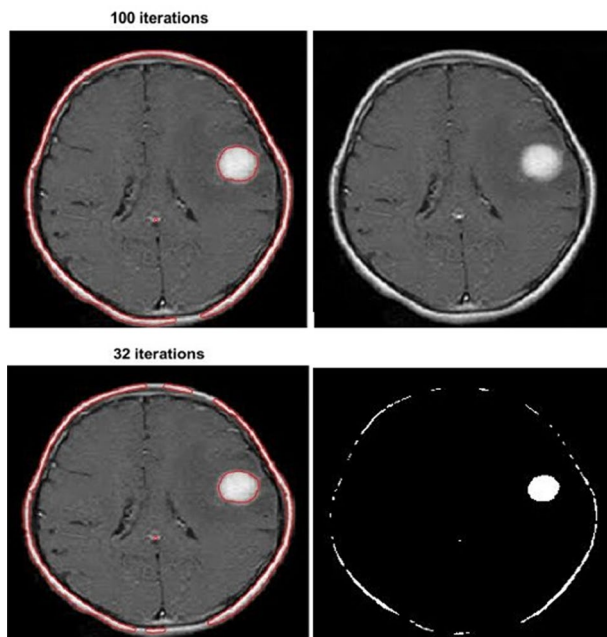


**Fig. 6** Original image (top left), the result of 100 iterations (top right), the result of initial curve of our method (bottom left), the result of 32 iterations (bottom right)

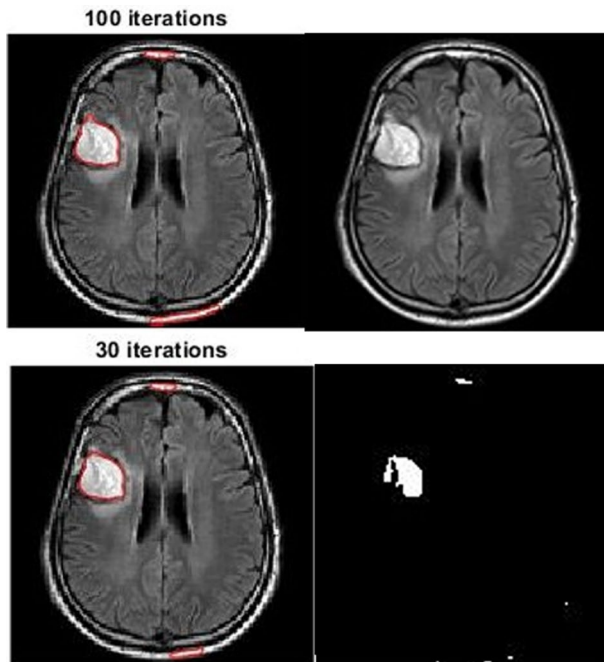


**Fig. 7** Original image (top left), the result of 100 iteration (top right), the result of initial curve of our method (bottom left), the result of 30 iteration (bottom right)

## 4.2 Qualitative evaluation

MRI scans have been then qualitative evaluated by analyzing the regions returned by the algorithm. The median filtering, applied to the diagonal neighboring of each pixels, led to soft edges. Moreover, the use of Canny edge detector to determine the initial curve, led to exact region of tumor and avoided false movements of the initial curve. Moreover, using variance value plus mean value in each region led to segmentation of inhomogeneous regions accurately as it can be shown in Figs. 5, 6, 7, 8, 9, 10, 11, and 12. In these figures, we have done the proposed method by 100 iterations, but what it can be seen in these figures is that, almost in 30 iterations the admissible results can be obtained.

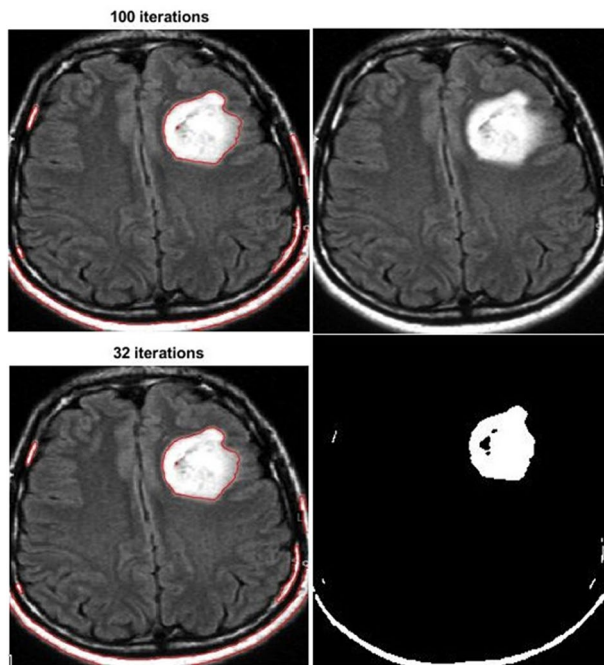


**Fig. 8** Original image (top left), the result of 100 iteration (top right), the result of initial curve of our method (bottom left), the result of 32 iteration (bottom right)

### 4.3 Comparison

For showing the effectiveness of the presented approach, it has been compared with the following baseline segmentation algorithms. Quantitative and qualitative analyses have been performed as described in the previous paragraphs.

- **CV model (CV):** It has been widely used in tasks related to image segmentation. It can be used only in images which have disjoint homogeneous subregions. However, this model does not work well with inhomogeneous images [45].
- **LBF model:** It uses each pixel intensity value to approximate the intensities of the neighbor pixels and expressed a local binary fitting energy with a kernel function. This model can be used in intensity-inhomogeneous images. But, the model has high computational complexity. Moreover, it is sensitive to the initial curve and setting parameters [47].
- **Local Fitted Image (LFI) Model:** It is defined based on image information in local neighborhood of pixels. This model can segment intensity-inhomogeneous



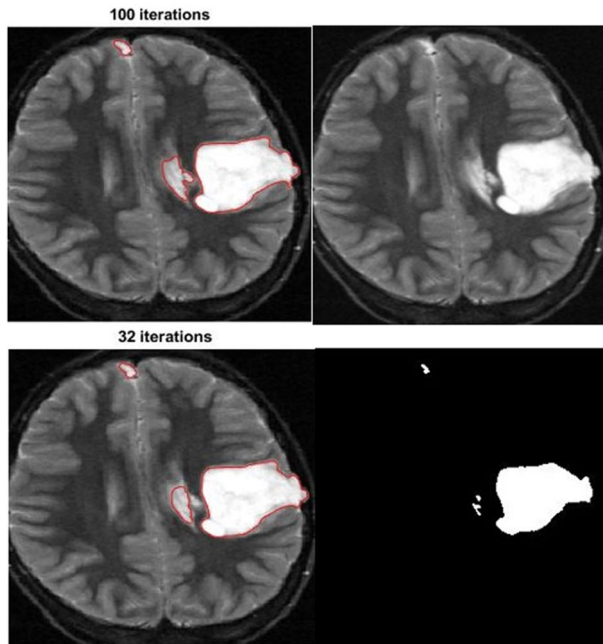
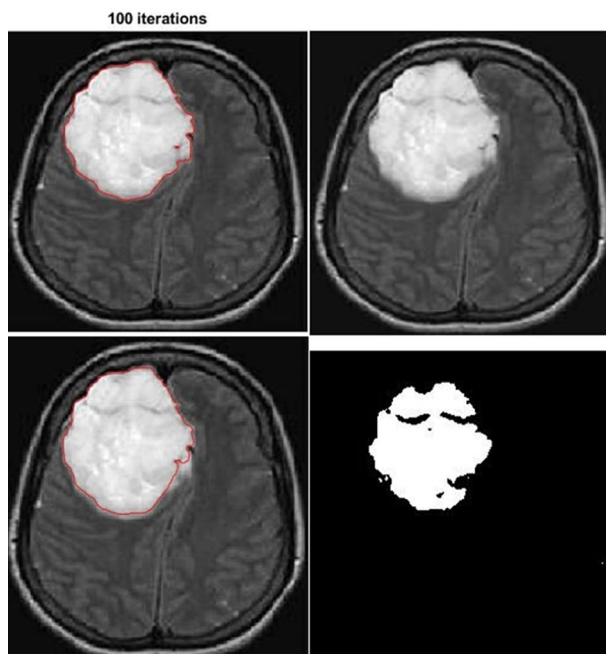


**Fig. 9** Original image (top left), the result of 100 iteration (top right), the result of initial curve of our method (bottom left), the result of 32 iteration(bottom right)

images. The LFI model is more effective than the LBF model. However, either LBF and LIF cannot deal with noisy and intensity-inhomogeneous images [36].

#### 4.4 Discussion

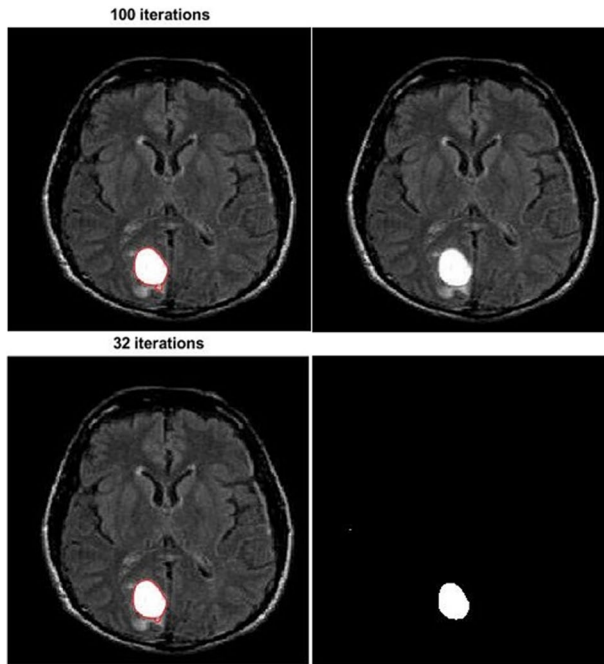
Table 1 reports a quantitative comparison of the introduced approach with state-of-the-art segmentation algorithms. Table 1 presents a comparison between the introduced method and the other segmentation models. We have compared accuracy, DSC, efficiency, and sensitivity in Table 1. Images from Whole Brain Atlas (Harvard University Medical School) datasets have been used. It is shown that the introduced technique returns high value of DSC. This suggests that it is able to accurately detect tumor regions and to return exact curve evaluation. Moreover, as it can be shown in Figs. 3 and 4, the proposed method is accurate in determining tumor region rather than previous active contours models. Based on the intensity values distribution, the tumor region can be extracted after some iterations as shown in Figs. 5, 6, 7, 8, 9, 10, 11, and 12.



**Fig. 10** Original image (top left), the result of 100 iteration (top right), the result of initial curve of our method (bottom left), the result of 16 iteration (bottom right)

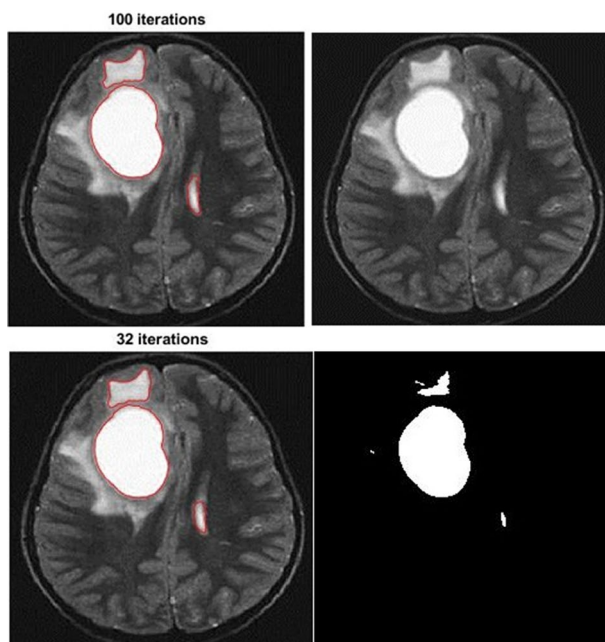
## 5 Conclusion

Image segmentation is a critical task in medical domain, since it is able to process medical images by detecting region of interest in them. For this reason, this methodology has been widely used to support physicians in their analyses. Automatic techniques, indeed are meant to support medical expert in their daily tasks, and not to replace them. In the case of image processing, the computational power of current technologies is able to analyze big amount of medical images in a short amount of time. Human expertise is then required to interpret the results automatically returned. In this work, a pipeline for image segmentation, based on level sets has been proposed, and its effectiveness has been evaluated on MRI scans of brain tumors. Results have shown that the introduced method overcomes state-of-the-art methodologies for segmentation, such as CV, LBF, and LIF. Moreover, it can be implemented in inhomogeneous regions. The use of Canny edge detector has led to determine initial curve automatically. Finally, the use of variance and mean values



**Fig. 11** Original image (top left), the result of 100 iteration (top right), the result of initial curve of our method (bottom left), the result of 32 iteration (bottom right)

in regions led to acceptable movements of curves. The proposed method for tumor segmentation can work very well specially the tumor is focused in a region. Also it can work well when there are more tumors regions with different variances. But, when the regions have variance values close to each other,  $\mu$  and  $\lambda$  values must be set with great care. Future works will be addressed to use more features in regions in order to better control the curve movement. Moreover, further works will aim to combine the proposed approach with deep learning algorithms, to extract the exact regions of tumor. Finally, the proposed approach will be applied in multiscale domains and multiphase methods based on active contours will be developed.



**Fig. 12** Original image (top left), the result of 100 iteration (top right), the result of initial curve of our method (bottom left), the result of 32 iteration (bottom right)

**Table 1** Quantitative comparison of the considered methods

Algorithm	DSC	Accuracy	Sensitivity	Specificity
Proposed method	0.997	0.988	0.978	0.995
CV	0.780	0.930	0.968	0.994
LBF	0.973	0.949	0.953	0.982
LIF	0.949	0.912	0.958	0.981

**Data Availability** The datasets analyzed during the current study are available in the *Whole Brain Atlas dataset, Neoplastic Disease (brain tumor)* part, [www.med.harvard.edu/aanlib](http://www.med.harvard.edu/aanlib).

## Declarations

**Conflict of interest** The authors declare that they have no conflict of interest.

## References

1. Weller M, Wick W, Aldape K et al (2015) Glioma. *Nat Rev Dis Primers* 1:15017
2. Vlaardingerbroek MT, Boer JA (2013) *Magnetic resonance imaging: theory and practice*. Springer Science & Business Media
3. Hameurlaine M, Moussaoui A (2019) Survey of brain tumor segmentation techniques on magnetic resonance imaging. *Nano Biomed Eng* 11(2):178–191


4. Bajaj AS, Chouhan U (2020) A review of various machine learning techniques for brain tumor detection from mri images. *Curr Med Imag* 16(8):937–945
5. Magadza T, Viriri S (2021) Deep learning for brain tumor segmentation: a survey of state-of-the-art. *J Imag* 7(2):19
6. Lella E, Vessio G (2020) Ensembling complex network ‘perspectives’ for mild cognitive impairment detection with artificial neural networks. *Pattern Recogn Lett* 136:168–174
7. Mahdi M, Nasser A (2021) A three-stage shearlet-based algorithm for vessel segmentation in medical imaging. *Pattern Anal Appl*. <https://doi.org/10.1007/S10044-020-00915-3>
8. Siadat M, Aghazadeh N, Akbarifard F, Brismar H (2019) Joint image deconvolution and separation using mixed dictionaries. *IEEE Trans Image Process* 28(8):3936–3945
9. Cigaroudy LS, Aghazadeh N (2017) A new multiphase segmentation method using eigenvectors based on k real number. *Circuits Syst Signal Process* 36(4):1445–1454. <https://doi.org/10.1007/S00034-016-0359-7>
10. Cigaroudy LS, Aghazadeh N (2017) A multiphase segmentation method based on binary segmentation method for Gaussian noisy image. *Signal Image Video Process* 11(5):825–831. <https://doi.org/10.1007/S11760-016-1028-9>
11. Aghazadeh N, Akbarifard F, Ladan SC (2016) A restoration-segmentation algorithm based on flexible Arnoldi-Tikhonov method and curvelet denoising. *Signal, Image Video Process* 10(5):935–942. <https://doi.org/10.1007/S11760-015-0843-8>
12. Cigaroudy LS, Aghazadeh N (2022) A Binary-Segmentation algorithm based on shearlet transform and eigenvectors, 2nd International Conference on Pattern Recognition and Image Analysis (IPRIA). <https://doi.org/10.1109/PRIA.2015.7161618>.
13. Narkhede HP (2013) Review of image segmentation techniques. *Int J Sci Modern Eng* 1(8):54–61
14. Caponetti L, Castellano G, Corsini V (2017) Mr brain image segmentation: a framework to compare different clustering techniques. *Information* 8(4):38
15. Liu T, Xu H, Jin W, Liu Z, Zhao Y, Tian W (2014) Medical image segmentation based on a hybrid region-based active contour model. *Comput Math Methods Med* 2014:1–10. <https://doi.org/10.1155/2014/890725>
16. An J-H, Chen Y (2007) Region based image segmentation using a modified Mumford-Shah algorithm. In: *International conference on scale space and variational methods in computer vision*. Springer, pp 733–742
17. Muller S, Ochs P, Weickert J, Graf N (2016) Robust interactive multi-label segmentation with an advanced edge detector. In: *German conference on pattern recognition*. Springer, pp 117–128
18. Xiangyang X, Shengzhou X, Jin L, Song E (2011) Characteristic analysis of Otsu threshold and its applications. *Pattern Recognit Lett* 32(7):956–961
19. Mehndiratta A, Giesed F (2011) Brain tumor imaging. In book: *Diagnostic Techniques and Surgical Management of Brain Tumors*. <https://doi.org/10.5772/23507>
20. Khairandish MO, Sharma M, Jain V, Chatterjee JM, Jhanjhi NZ (2022) A Hybrid CNN-SVM threshold segmentation approach for tumor detection and classification of MRI brain images. *IRBM* 43(4):290–299
21. Sivakumar V, Janakiraman N (2020) A novel method for segmenting brain tumor using modified watershed algorithm in MRI image with FPGA. *Biosystems* 198:104226. <https://doi.org/10.1016/j.biosystems.2020.104226>
22. Daimary D, Mayur BB, Khwairakpam A, Debdatta K (2020) Brain tumor segmentation from MRI images using hybrid convolutional neural networks. *Proc Computer Sci* 167:2419–2428
23. Jaspin Jeba Sheela C, Suganthi G (2022) Automatic brain tumor segmentation from MRI using greedy snake model and fuzzy C-means optimization. *J King Saud Univ- Computer Inf Sci* 34(3):557–566
24. Amin J, Sharif M, Gul N, Yasmin M, Shad SA (2020) Brain tumor classification based on DWT fusion of MRI sequences using convolutional neural network. *Pattern Recognit Lett* 129:115–122
25. Mumford DB, Shah J (1989) Optimal approximations by piecewise smooth functions and associated variational problems. *Commun Pure Appl Math* 25:46
26. Bickey KS, Vansh K, Rohan R, Sakil A, Anshul S (2020) Evaluation and comparative study of edge detection techniques. *IOSR J Computer Eng* 22(5):06–15
27. Sert E, Avci D (2019) A new edge detection approach via neutrosophy based on maximum norm entropy. *Expert Syst Appl* 115:499–511

28. Sangeetha D, Deepa P (2019) FPGA implementation of cost-effective robust Canny edge detection algorithm. *J Real-Time Image Process* 16(4):957–970. <https://doi.org/10.1007/s11554-016-0582-2>
29. Kim W, Kim C (2012) Active contours driven by the salient edge energy model. *IEEE Trans Image Process* 22:1667–1673
30. Lecellier F et al (2010) k Region-based active contours with exponential family observations. *J Math Imag Vis* 36:28
31. Cohen R (2011) The chan-vese algorithm. <http://arxiv.org/abs/1107.2782>
32. Osher S, Sethian JA (1988) Fronts propagating with curvature-dependent speed: Algorithm based on Hamilton-Jacobi formulations. *J Comput Phys* 79(1):12–49
33. Ali H, Badshah N, Chen K, Khan G (2016) A variational model with hybrid images data fitting energies for segmentation of images with intensity inhomogeneity. *Pattern Recognit* 51:27–42
34. Wang X, Huang D, Xu H (2010) An efficient local Chan-Vese model for image segmentation. *Pattern Recognit* 43(3):603–618
35. Mabood L, Ali H, Badshah N, Ullah T (2015) Absolute median deviation based a robust image segmentation model. *J Inf Commun Technol* 9(1):13–22
36. Zhang K, Song H, Zhang L (2010) Active contours driven by local image fitting energy. *Pattern Recognit* 43(4):1199–1206
37. Jayadevappa D, Kumar S, Murty D (2011) Medical image segmentation algorithms using deformable models: a review. *IETE Tech Rev* 28(3):248–255
38. Li C, Wang X, Eberl S, Fulham M, Feng D (2013) Robust model for segmenting images with/without intensity inhomogeneities. *IEEE Trans Image Process* 22(8):3296–3309
39. Wang B, Gao X, Tao D, Li X (2014) A nonlinear adaptive level set for image segmentation. *IEEE Trans Cybern* 44(3):418–428
40. Wang H, Liu M (2013) Active contours driven by local gaussian distribution fitting energy based on local entropy. *Int J Pattern Recognit Artif Intell* 27(6):1073–1089
41. Chen F, Yu H, Hu R (2013) Shape sparse representation for joint object classification and segmentation. *IEEE Trans Image Process* 22(3):992–1004
42. Mylona E, Savelonas M, Maroulis D (2014) Automated adjustment of region-based active contour parameters using local image geometry. *IEEE Trans Cybern* 44(12):2757–2770
43. Yang X, Gao X, Li J, Han B (2014) A shape-initialized and intensity-adaptive level set method for auroral oval segmentation. *Inf. Sci.* 277(2):794–807
44. Hong-Kai ZT, Chan B, Merriman SO (1996) A variational level set approach to multiphase motion. *J Comput Phys* 127(1):179–195
45. Chan TF, Vese LA (2001) Active contours without edges. *IEEE Trans Image Process* 10(2):266–277
46. Li Bing N, Chui Chee K, Chang S, Ong Sim H (2011) Integrating spatial fuzzy clustering with level set methods for automated medical image segmentation. *Computers Biol Med* 41(1):1–10
47. Li C, Kao C-Y, Gore JC, Ding Z (2007) Implicit active contours driven by local binary Fitting energy. In 2007 IEEE Conference on Computer Vision and Pattern Recognition, pp 1–7
48. Li C, Kao C-Y, Gore JC, Ding Z (2008) Minimization of region scalable fitting energy for image segmentation. *IEEE Trans Image Process* 17(10):1940–1949
49. Canny J (1986) A computational approach to edge detection. *IEEE Trans Pattern Anal Mach Intell* 6:679–698
50. <https://www.med.harvard.edu/aANlib/home.html>
51. Hunderi AH, Karunakaran N (2013) Segmentation of medical image data using level set methods, master thesis, department of computer and information science, Norwegian University of Science and Technology

**Publisher's Note** Springer Nature remains neutral with regard to jurisdictional claims in published maps and institutional affiliations.

Springer Nature or its licensor (e.g. a society or other partner) holds exclusive rights to this article under a publishing agreement with the author(s) or other rightsholder(s); author self-archiving of the accepted manuscript version of this article is solely governed by the terms of such publishing agreement and applicable law.

## Authors and Affiliations

Nasser Aghazadeh<sup>1</sup>  · Paria Moradi<sup>1</sup> · Giovanna Castellano<sup>2</sup> · Parisa Noras<sup>1</sup>

✉ Nasser Aghazadeh  
aghazadeh@azaruniv.ac.ir

Paria Moradi  
pmoradi@azaruniv.ac.ir

Giovanna Castellano  
giovanna.castellano@uniba.it

Parisa Noras  
p.noras@azaruniv.ac.ir

<sup>1</sup> Image Processing Laboratory, Department of Mathematics, Azarbaijan Shahid Madani University, Tabriz, Iran

<sup>2</sup> Department of Computer Science, University of Bari, Bari, Italy